Inorganic Chemistry

Article

pubs.acs.org/IC

Dioxygen Oxidation Cu(II) → Cu(III) in the Copper Complex of *cyclo*(Lys-D-His-β-Ala-His): A Case Study by EXAFS and XANES Approach

Alessandro Pratesi,[†] Gabriele Giuli,[‡] Maria Rita Cicconi,[‡] Stefano Della Longa,[§] Tsu-Chien Weng,[∥] and Mauro Ginanneschi[†,*]

[†]Laboratory of Peptide & Protein Chemistry & Biology, Department of Chemistry "Ugo Schiff", University of Firenze, Via della Lastruccia 13, 50019 Sesto Fiorentino (FI), Italy

[‡]Dipartimento di Scienze della Terra, University of Camerino, Via Gentile III da Varano, 62032 Camerino, Italy

[§]Dipartimento di Medicina Sperimentale, Università dell'Aquila, Via Vetoio, loc. Coppito, 67100, L'Aquila, Italy

[∥]European Synchrotron Radiation Facility, ESRF, F-38043 Grenoble, France

Supporting Information

ABSTRACT: A former spectroscopic study of Cu(II) coordination by the 13-membered ring cyclic tetrapeptide *c*(Lys-D-His-β-Ala-His) (DK13), revealed the presence, at alkaline pH, of a stable peptide/Cu(III) complex formed in solution by atmospheric dioxygen oxidation. To understand the nature of this coordination compound and to investigate the role of the His residues in the Cu(III) species formation, Cu K-edge XANES, and EXAFS spectra have been collected for DK13 and two other 13-membered cyclo-peptides: the diastereoisomer *c*(Lys-His-β-Ala-His) (LK13), and *c*(Gly-β-Ala-Gly-Lys) (GK13), devoid of His residues. Comparison of pre-edge peak features with those of Cu model compounds, allowed us to get information on copper oxidation state in two of the three peptides, DK13 and GK13: DK13 contains only Cu(III) ions in the experimental conditions, while GK13 binds only with Cu(II). For LK13/Cu complex, EXAFS spectrum suggested and UV−vis analysis confirmed the presence of a mixture of Cu(II) and Cu(III) coordinated species. Theoretical XANES spectra have been calculated by means of the MXAN code. The good agreement between theoretical and experimental XANES data collected for DK13, suggests that the refined structure, at least in the first coordination shell around Cu, is a good approximation of the DK13/Cu(III) coordination species present at strongly alkaline pH. All the data are consistent with a slightly distorted pyramidal CuN_4 unit, coming from the peptide bonds. Surprisingly, the His side-chains seemed not involved in the final, stable, Cu(III) scaffold.

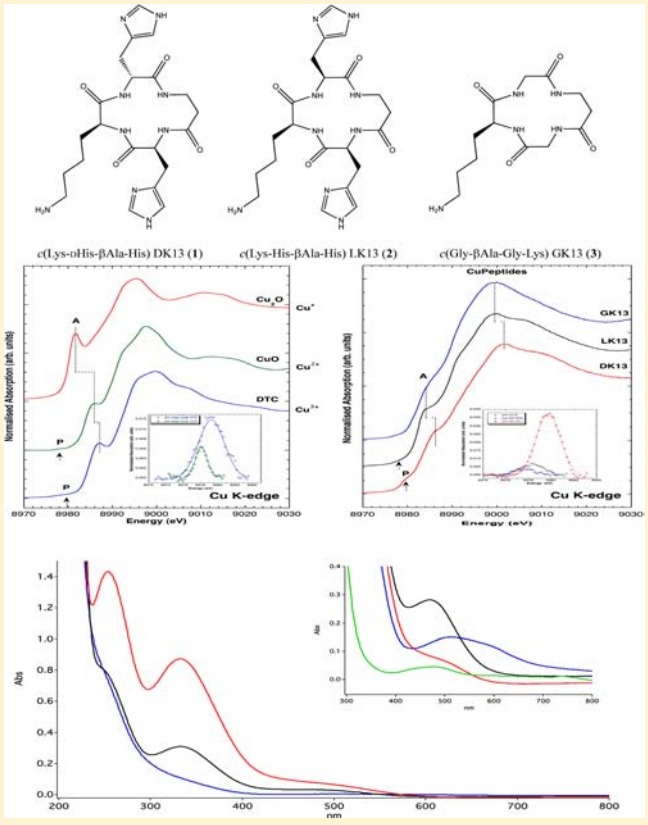

INTRODUCTION

The study of the behavior of acyclic and cyclic peptides is growing in importance because of the actions that many of these substances display, working like hormones, antibiotics, enzymes or metals carrier molecules. In addition, the coordination geometry of metal ions in peptides is of great interest, mimicking the complexation sites in macromolecular ligands like proteins. Among the metallic oligo-elements necessary to the human life, the copper, even not the most abundant one, is however one the most active in the biochemical pattern, and it is deeply involved in the mechanism of the cellular redox reactions. Copper ions, in fact, are found in the active pocket of a versatile group of redox catalysts like citocrome-c oxidase, galactose oxidase, or superoxide dismutase (SOD) and play a fundamental role in the cell protection from

Received: July 12, 2011
Published: July 19, 2012

   dx.doi.org/10.1021/ic201469h | *Inorg. Chem.* 2012, 51, 7969−7976

Chart 1. Three Cyclopeptides Studied

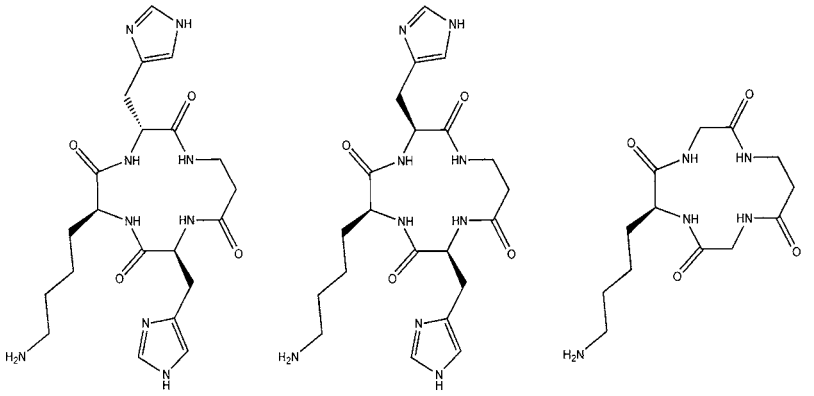

c(Lys-D-His-β-Ala-His) DK13 (**1**) *c*(Lys-His-β-Ala-His) LK13 (**2**) *c*(Gly-β-Ala-Gly-Lys) GK13 (**3**)

ROS dangerous activity. Moreover, Cu(II) ion is the most tightly bound metal ion in the chelating centers of biological molecules, which accounts for the fact that the copper present in living cells is almost entirely coordinated by peptides or proteins. Notably, copper(II) is stored at high levels in the brain cells through the human prion protein (PrP), where it is bonded to four repeats of the eight-residue sequence PHGGGWGQ by one imidazole and two amide nitrogens, at neutral pH value.[1] A correct homeostasis of copper is therefore essential for the right physicochemical equilibrium of the organism: the required amount of copper(II) ion assumed by the diet lies in the range of 1.5−3.0 mg pro die. The control of toxicity of copper is based on mechanisms related to redox enzymes function, extra- and intracellular chelation and a fine-tuning of the transmembrane transport. Hence, the effective plasma transport of copper is also fundamental for the homeostasis of this metal and it is ensured by various proteins like ceruloplasmin and serum albumin. Noteworthy, a significant fraction of Cu(II) is also bonded to low-weight peptide species which act as carriers in the biological fluids.[2] In His containing peptides and proteins, at the physiological pH values, Cu(II) is tightly bonded to the imidazole side-chain of the His residues, which are able to coordinate copper ions since acidic pH. Peptide bonds could be also deprotonated already at pH 7 by Cu(II) coordination, often with the simultaneous involvement of the *N*-3 imidazole atom to form penta- or hexaatomic-cycles.[1] Moreover, cyclopeptides of suitable size are generally prone to coordinate Cu(II) stronger than the parent linear oligopeptides. That is true when cyclotetrapeptides with the −His-Xaa-His− motif are implicated in the coordination.[3] This prompted us to undertake a systematic study on the speciation of Cu(II) complexes in several oligopeptides containing histidine residues, especially cyclic peptides of different cavity size.[4−9] The coordination of Cu(II) ion with these molecules was studied in a large range of pH values by potentiometric and spectroscopic methods. This allowed us to detect the principal donor sets and to determine the structure of the most abundant species in equilibrium. In all the studied peptides, linear and cyclic as well, we were dealing with peptide/copper(II) complexes. In particular, *c*(Lys-D-His-Gly-His) and *c*(β^3homoLys-D-His-β-Ala-His), containing 12- and 14-atoms rings, respectively, gave well-defined $CuH_{-4}L$ species at strong alkaline pH, with 4N equatorial donor set around Cu(II) coordination and the involvement of the Im nitrogens, affording octahedral-like structures.

Recently, we prepared a new 13-member cyclotetrapeptide, containing the D-His-Xaa-L-His motif *c*(Lys-D-His-β-Ala-His) (DK13), (**1**). Surprisingly, preliminary studies carried out by optical spectroscopy, NMR, MS, and electrochemistry methods, suggested that, in strongly alkaline aqueous solutions, the added Cu(II) was almost completely transformed in Cu(III) species through the action of dioxygen dissolved in the solution.[10] Notably, the ligand *c*(Gly-β-Ala-Gly-Lys) (GK13) (**3**) containing a cycle of the same size but devoid of His residues, appeared to bond only Cu(II) ions in the same conditions by UV−vis inspection. We noticed also that the stabilization effect obtained by peptide (**1**) on the potent oxidizing agent Cu(III) is by far strongest than that reported for the related Cu(III) complex with the 14-membered peptide *c*(β-Ala-Gly-β-Ala-Gly).[11] Attempts to clarify the DK13/Cu(III) complex structure by means of usual X-ray diffraction analysis on powdered samples failed. This prompted us to use the more powerful synchrotron radiation method for investigating the nature of the copper complexes of this cyclopeptide. In the following, we report an enhanced Cu K-edge XANES and EXAFS structural study of the DK13/Cu(III) complex, carried out at the ESRF facility of Grenoble on solid state samples obtained by liophylisation of strong alkaline solutions. Similarly, X-rays data for mixtures of Cu(II) with the diastereoisomer peptide *c*(Lys-His-β-Ala-His) (LK13) (**2**) and with GK13 (**3**) were collected at ESRF and the results compared with those obtained for DK13.

EXPERIMENTAL SECTION AND DATA REDUCTION

Synthesis of the Cyclopeptides. Chloro-trityl resin (100−200 mesh) was from Novabiochem AG (Laufelfingen, Switzerland). All aminoacids, TBTU and HOBt are from Iris Biotech (Marktredwitz, Germany), HATU from ChemPep (Wellington, USA). Peptide-synthesis grade DMF was from Scharlau (Barcelona, Spain). HPLC-grade MeCN was purchased from Carlo Erba (Italy). Dry solvents were distilled immediately before use. All other chemicals were commercial compounds and were used as received. The solid-phase syntheses were performed on semiautomatic synthesizer (MultiSynTech − Germany). ^{1}H NMR spectra were recorded on a Varian Gemini 300 MHz or Varian Inova 400 MHz spectrometer in DMSO-d_6 or D_2O. Chemical shifts are reported in ppm (δ) downfield from tetramethylsilane. Electrospray ionization mass spectra (ESI-MS) were acquired on LCQ-Advantage ESI ion trap spectrometer (Thermo Finnigan) for positive and negative ions detection. The purity

dx.doi.org/10.1021/ic201469h | *Inorg. Chem.* 2012, 51, 7969−7976

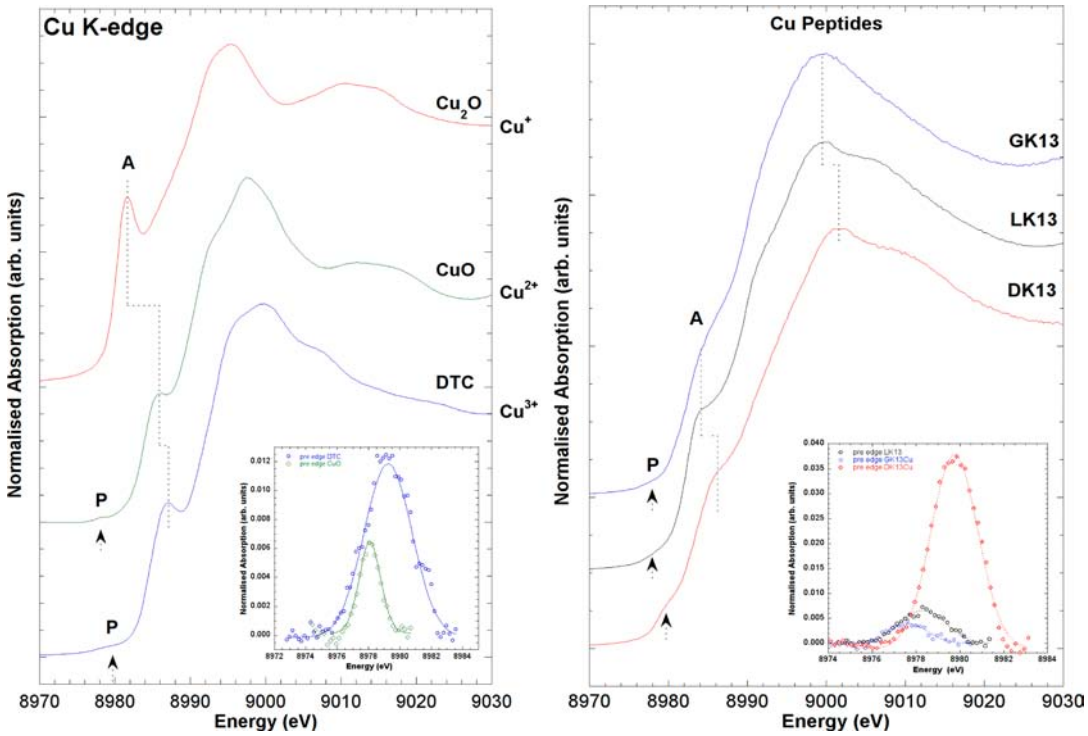

Figure 1. XANES spectra of Cu model compounds with known oxidation state (left panel) and the peptides under study (right panel).

of the final compounds was checked by HPLC and by combustion analysis, performed on a Perkin-Elmer 240 C elemental analyzer.

The syntheses of DK13 (**1**) and GK13 (**3**) have been previously reported.[10] Briefly, linear tetrapeptide precursor of DK13 was prepared following the SPPS method and using the orthogonal Fmoc/Trt/allyl protection scheme on a trityl type resin, by anchoring the imidazole side-chain. The chain elongation was achieved according to SPPS standard protocol, and the on-resin cyclic compound was obtained in the pseudodilution conditions, forming the peptide bridge by TBTU/DIPEA method in DMF. The cyclization yield was >90%, without the presence of oligomer byproducts. The synthesis and cyclization were performed as reported for DK13. Peptides cleavage from the resin and deprotection of the aminoacids side chains were carried out with TFA/H_2O/TIS (95:2.5:2.5) while the crude cyclic compounds were both purified by RPC_{18}–HPLC and characterized by LC-ESI-MS. The solvent systems used for gradients were A (0.1% TFA in H_2O) and B (0.1% TFA in CH_3CN).

Synthesis of (3*S*,6*S*,9*S*)-3,9-Bis((1*H*-imidazol-4-yl)-methyl)-6-(4-aminobutyl)-1,4,7,10-tetraazacyclotridecane-2,5,8,11-tetraone (LK13) (2). The synthesis started from Fmoc-His(trityl-resin)-OAl (500 mg, 0.46 mmol/g). Fmoc deprotection was performed by 20% piperidine in DMF (2 × 5 mL) for 15 min. Amino acids residues (β-Ala; His and Lys, respectively) were then introduced according to the TBTU/HOBt/NMM method for the active esters formation. The coupling reactions were performed by using excess of the amino acids, HOBt and TBTU (4 equiv) and of NMM (8 equiv) in DMF, under vortex mixing for 40 min. After deprotection, the cyclization was performed as reported for compound **1**. The crude LK13 was prepurified by solid phase extraction (SPE) and semipreparative RP-HPLC (0% to 20% of B in 30 min.) giving **2** (65 mg, 16% overall yield). Analytical HPLC (3% to 20% of B in 5 min.; flow 600 μL/min): t_R = 1.47 min; ESI-MS: m/z calcd $[M+H]^+$, 474.53, found 474.42. Elemental analysis. Found: C, 39.09; H, 4.46; N, 15.21%. Calculated for $C_{21}H_{31}N_9O_4 \cdot 1H_2O \cdot 3TFA$: C, 38.90; H, 4.35; N, 15.12%. The preparations of the copper–peptide complexes for XANES and EXAFS experiments are described in Supporting Information.

Spectroscopic Investigations. UV–vis spectroscopy data have been acquired with a Varian Cary 50 instrument, using a mixture of cyclopeptides **1**, **2**, and **3**, respectively (0.15 mM) and 0.1 mM Cu(II), in air saturated aqueous solutions, at pH 12.2, in the range from 200 to 800 nm.

X-ray absorption spectroscopy (XAS) data have been collected at the ID26 beamline of the ESRF storage ring (Grenoble, F) with ring current ranging from 90 to 60 mA, on solid samples obtained by liophylisation of freshly prepared aqueous solutions (cyclopeptide/copper 1:0.9) at high pH values. Radiation was monochromatised by means of a double-crystal Si (311) monochromator to achieve high-energy resolution at the Cu K-edge. Beam size at the sample was 250 × 1000 μm. Cu K-edge XANES and EXAFS spectra were acquired in fluorescence mode monitoring the emitted fluorescence signal with a high-purity multielement Ge detector. XAS data were collected in quick-scan mode by simultaneously scanning the monochromator angle and the undulator gap with a typical energy step of 0.2 eV and counting about 160 ms per point. In order to reduce radiation induced damage of the peptide samples, spectra have been collected at 10 K in a He cryostat, and the intensity of the incident radiation at the sample has been adjusted by means of Al filters. Preliminary time scans allowed to ascertain that the samples suffered no damage within 1300 s exposure to the X-ray beam. For each sample 1000 s long spectra have been acquired at different sample positions in order not to alter the sample. Average of 10 to 60 scans, depending on sample Cu

dx.doi.org/10.1021/ic201469h | *Inorg. Chem.* 2012, 51, 7969–7976

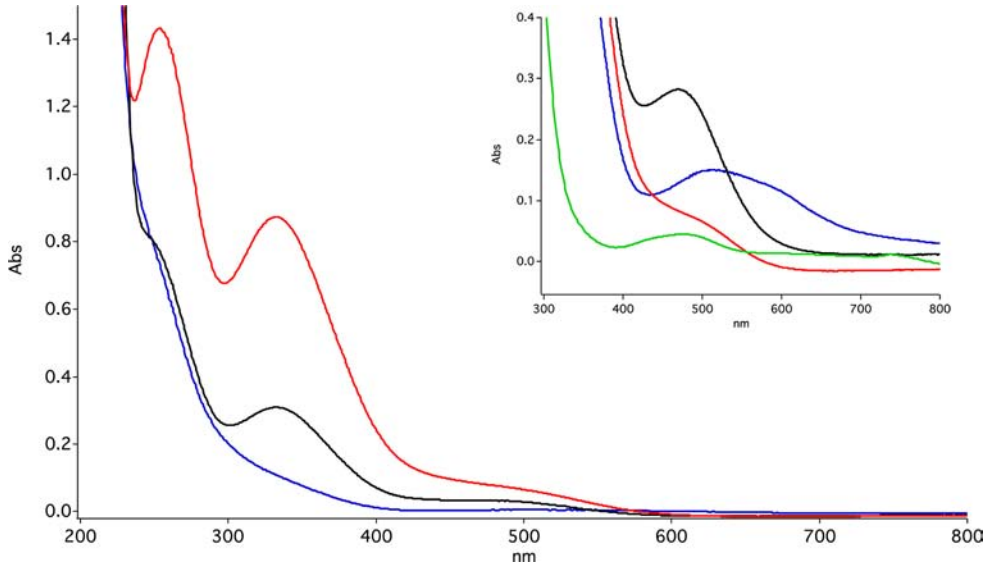

Figure 2. UV−vis spectral trend for DK13/Cu (red line), LK13/Cu (black line) and GK13/Cu (blue line) in acqueous solutions at pH 12.2. Peptides concentration 0.15×10^{-3} M; ligand to metal ratio 1:0.9. In the inset are reported the d−d transitions because of the presence of Cu(II) in LK13 (black line), GK13 (blue line), and $c(\beta^3$homoAsp-DHis-βAla-His) (green line) complexes. Peptides concentration = 1.5×10^{-3} M; ligand to metal ratio = 1:0.9.

concentration, allowed to obtain a good signal-to-noise ratio for all the samples.

Experimental XANES spectra were corrected by background subtraction with a linear function and then normalized for atomic absorption on the average absorption coefficient of the spectral region from 9030 to 9210 eV. Energy was calibrated against a standard of Cu metal (8979 eV). The threshold energy was taken as the first maximum of the first derivative of the spectra, whereas peak positions were obtained by calculating the second derivative of the spectra. Pre-edge peak analysis was carried out following the same procedure found in Wilke et al.[12] The pre-edge peak was fitted by a sum of pseudo-Voigt function, and the integrated intensities along with centroid energies were compared with those of the standards analyzed here and others from the literature in order to extract information on Cu oxidation state and coordination number in the samples studied.

EXAFS data reduction and analysis was done by means of the GNXAS package (Filipponi & Di Cicco, 2000).[13] This program extracts χ(k) signal from the raw spectrum without performing Fourier filtering and thus avoiding possible biases deriving from incorrect background subtraction. The theoretical amplitudes and phase shifts are calculated ab initio according to the Muffin-Tin approximation. The Hedin−Lundqvist complex potential[14] was used for the exchange-correlation potential of the excited state. The amplitude reduction factor (S_0^2) has been fixed to 0.85.

XANES analysis has been carried out by using the MXAN program[15] working in the frame of the one-electron, multiple scattering theory using a complex, "Muffin-Tin" molecular potential.[16] The real part of the exchange term of the potential was calculated using the Hedin−Lundqvist energy-dependent potential[16] while the imaginary part of the potential, taking into account all of the inelastic losses, was mimicked by a phenomenological method previously described in detail.[16,17] Starting atomic coordinates were first calculated according to a DFT minimization; the XANES spectrum was then calculated using the real Hedin−Lundqvist potential convoluted with a broadening function, with a width Γ given by $\Gamma = \Gamma_c + \Gamma(E)$. The constant part Γ_c includes contributions from the core-hole lifetime (1.5 eV, Lorentzian convolution) and the experimental resolution (0.6−0.8 eV, Gaussian convolution), while the energy dependent term $\Gamma(E)$ (Lorentzian convolution) represents the inelastic processes. $\Gamma(E)$ follows the universal functional form related to the mean free path in a solid,[18] but it is also refined during the procedure. Structural optimization was performed by minimizing the χ^2 function of the theoretical vs experimental fit in the space of two structural parameters, that is, the first (4 nitrogens) and second (8 carbons) coordination shell.

RESULTS AND DISCUSSION

Pre-edge Analysis. In Figure 1 are shown the XANES spectra of representative Cu model compounds with known oxidation state and the peptides under study. As the metal K-edge structures vary according to number, type, and geometric arrangements of ligands, as well as the metal oxidation state, comparison of the peptide spectra with those of model compounds can allow to get information on the oxidation state and structural surrounding of the studied metal (i.e., Cu).

It is apparent a general shift to higher energy of the absorption threshold of the model compound spectra with increasing Cu oxidation state from Cu(I) to Cu(III). Also a peak labeled A in the edge region shifts to higher energy with increasing Cu oxidation state. Moreover, a peak in the pre-edge region (peak P) is absent in the Cu(I) model compounds whereas is present in Cu(II) and Cu(III) compounds. This peak, often referred as pre-edge peak, is related to a 1s to 3d electronic transition in the photoabsorbing atom (in this case Cu) and is a direct probe of the unfilled d orbital population.[19,20] The observed variations of edge positions and pre-edge peak position and intensities have been already observed in a number of systems of both organic and inorganic nature.[21−24] However, the quantitative interpretation of XANES spectra is sometimes rendered difficult because of the complexity of multiple scattering paths involved and

dx.doi.org/10.1021/ic201469h | Inorg. Chem. 2012, 51, 7969−7976

because of the high number of factors affecting the shape of the XANES region. In this respect, the pre-edge peak can be solely an indication of the metal oxidation state.[25] The background subtracted pre-edge peak is shown in the inset of Figure 1 for both the model compounds (left panel) and peptides (right panel). The energy position of this peak can be a precise indication of the Cu oxidation state: while it is absent in Cu(I) compounds, it is present at ca. 8978 eV for most Cu(II) model compounds. Its shift to higher energy and increase in integrated intensity in the case of Cu(III) compounds. The Cu(III) model compound shown here [ditellurate cuprate(III), DTC] display a pre-edge peak centroid at 8979.3 ± 0.3 eV with an integrated intensity of 0.044. Comparison of peptide pre-edge peak data with those of model compounds can probe Cu oxidation state in the studied peptide samples. Accurate analysis of pre-edge peak data of the peptide samples allowed to ascertain the presence of Cu(III) in cyclopeptide **1** and of Cu(II) in cyclopeptide **3** samples, respectively. In particular, while the pre-edge peak of the GK13/Cu sample is perfectly compatible with those of divalent Cu model compounds analyzed here and reported in the literature, the pre-edge peak of DK13 spectrum display an energy (8979.8 eV) compatible to that of the DTC shown here (and with other data from the literature[22]) but has an higher integrated intensity (0.095) than the DTC, possibly due to a less centrosymmetric geometrical environment around Cu than in the DTC. The small increase in the pre-edge intensity in LK13/Cu sample (**2**) could indicate a small amount of Cu(III), or could merely be due to change in site symmetry. To clarify wich of the two hypotheses was correct, we investigated the presence of a Cu(III) complex in LK13/Cu by means of the UV−vis spectroscopy.

UV−vis Analysis. The comparison of UV−vis spectra of the three peptide/copper complexes, reported in Figure 2, strongly supports the XANES data. The DK13/copper spectrum shows two strong absorptions at λ_{max} 252 and 332 nm which can be attributed to LMCT bands diagnostic for Cu(III)/peptide square planar complexes.[10,26] (Table1). The

Table 1. Spectroscopic Data for the Three Peptide/Cu Complexes at 20 °C[a]

peptide/Cu complex	λ_{max} (nm)	ε (cm^{-1} M^{-1})
DK13	254[b]	9570
	332[b]	5823
	~510[c]	
LK13	249[b]	
	332[b]	
	~470[c]	
GK13	~520[c]	101

[a]The ligand concentration was 1.5 × 10^{-3} M. Ligand to metal ratio was 1:0.9. [b]N^- → Cu(III) CT bands; [c]Cu(II) d−d transitions.

very weak and broadened absorbance at ~510 nm cannot be attributed to a Cu(III) CT (the $\varepsilon \cong 380$ would be low) and suggests the presence of a residual Cu(II) complex. On the contrary, the spectral pattern of compound (**3**)/Cu(II) solution does not show anywhere the characteristic maxima at ~250 and ~330 nm but only a broad absorption at about 520 nm whose low molar absorptivity (101 M^{-1} cm^{-1}) is in agreement with a d-d transition of a coordinated Cu(II) ion, probably due to peptide $4N^-$ donor set like the smaller *c*(HGHK) (λ_{max} 529 nm, pH 12.8).[8] Conversely, the LK13/Cu spectral pattern shows a shoulder at about 250 nm and a maximum just at 332 nm, well in accordance with the occurrence of the peptide/Cu(III) species. The simultaneous presence of the broad absorption at ~470 nm, assignable to the d-d transition of a Cu(II) coordinated species,[9] confirms the largely incomplete oxidation of Cu(II) ions. For the sake of clarity, the inset of Figure 2 reports also the UV−vis spectrum of the *c*(β^3homoAsp-DHis-βAla-His)/Cu(II) complex at pH 11 (λ_{max} 474 nm, unpublished data). Quantitative analysis of Cu(III)/Cu(II) ratios cannot be reasonably carried out at this stage but qualitative results seem in good agreement with the pre-edge analysis obtained by XANES.

EXAFS Analysis. In Figure 3 are shown the experimental (open symbols), theoretical (solid lines), and residual EXAFS signals of the DK13/Cu(III) and GK13/Cu(II) samples. The theoretical signals have been calculated starting from a simplified model structure reproducing the 13-element ring and neglecting the imidazole side chains contributions. The signals have a low intensity and are almost completely dumped in the high-energy region. The Fourier transforms of the EXAFS signals confirm that there are no important contributions from distances farther than 4 Å.

The theoretical contributions to the EXAFS signals from each shell of the model structure are shown in Figure 4 for two peptides: The most important contributions comes from the 4 N atoms bonded to Cu and from the 6 nearest C atoms. The other three contributions refer to longer Cu−C distances within 4.0 Å from the Cu site. The EXAFS derived Cu−N distances are sensibly shorter in the DK13/Cu sample relative to GK13/Cu (1.78 ± 0.02 Å and 1.91 ± 0.02 Å respectively). The shorter distance (1.78 Å for DK13) is consistent with other Cu(III)-N distances found in the literature[22] and is thus a further confirmation of the presence of trivalent copper in this peptide. On the other hand, the Cu−N distance found for GK13/Cu (1.91 Å) compares well with known values for divalent copper.[22,27]

XANES Analysis. Theoretical XANES spectra of DK13 and GK13 copper complexes are shown in Figure 5, left frame. Whereas, as expected, prepeak P cannot be reproduced, the main features A, B, C, D of the edge, and their changes going from GK13/Cu to DK13/Cu are satisfactorily reproduced in the one-electron, multiple scattering scheme adopted by the MXAN program. In particular the observed blue-shift of the spectrum going from the cuprous to cuprate compound correspond to a decrease of the average first shell distance. In the right frame, the Theoretical vs Experimental fit concerning DK13 and GK13 copper complexes, is displayed.

In this figure, the experimental spectra have been shifted by ~8985 eV to lower energy to match the theoretical spectra. The fits include the first and second shell average distances. Electron damping and all the anelastic losses are taken into account by a phenomenological broadening function (see the Supporting Information). Because of the poor approximation used for this function, the details of the edge features (at 0−20 eV) are smeared out in the theoretical spectra, however they are unessential for the fit results that are based on the simulation of a much longer energy range. The results of the MXAN fits are in quite agreement with the EXAFS analysis (see Table 2). The Cu−N average distance is 1.80 ± 0.04 Å for DK13 and 1.91 ± 0.02 Å for GK13, while the average second shell Cu−C distance (calculated on the eight nearest carbon atoms) is 2.84 ± 0.08 and 2.94 ± 0.02 Å, respectively.

dx.doi.org/10.1021/ic201469h | Inorg. Chem. 2012, 51, 7969−7976

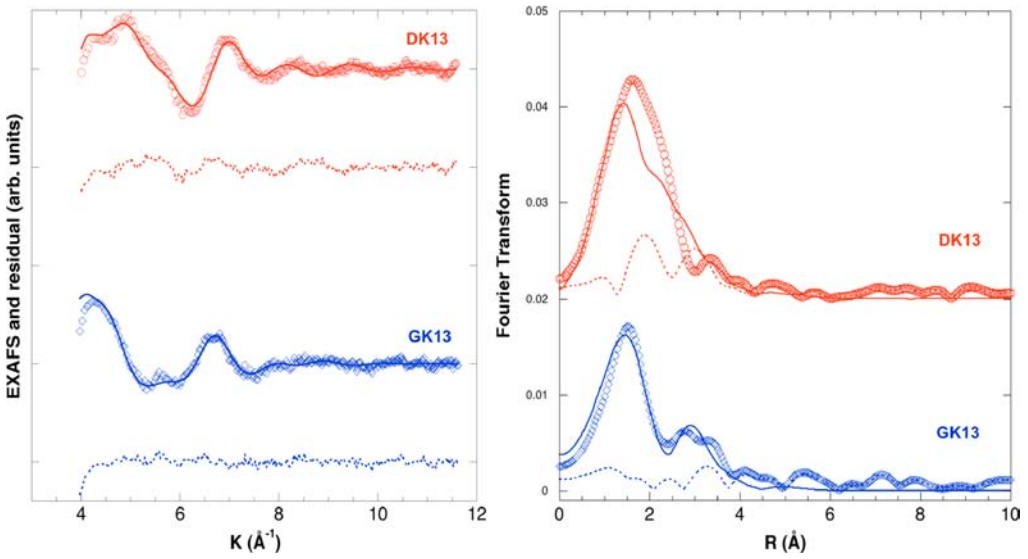

Figure 3. Cu K-edge EXAFS signals (left panel) and Fourier transforms (right panel) of Cu(III) (red line) and Cu(II) (blue line) peptide samples (○, EXAFS; — theoretical; ··· residual).

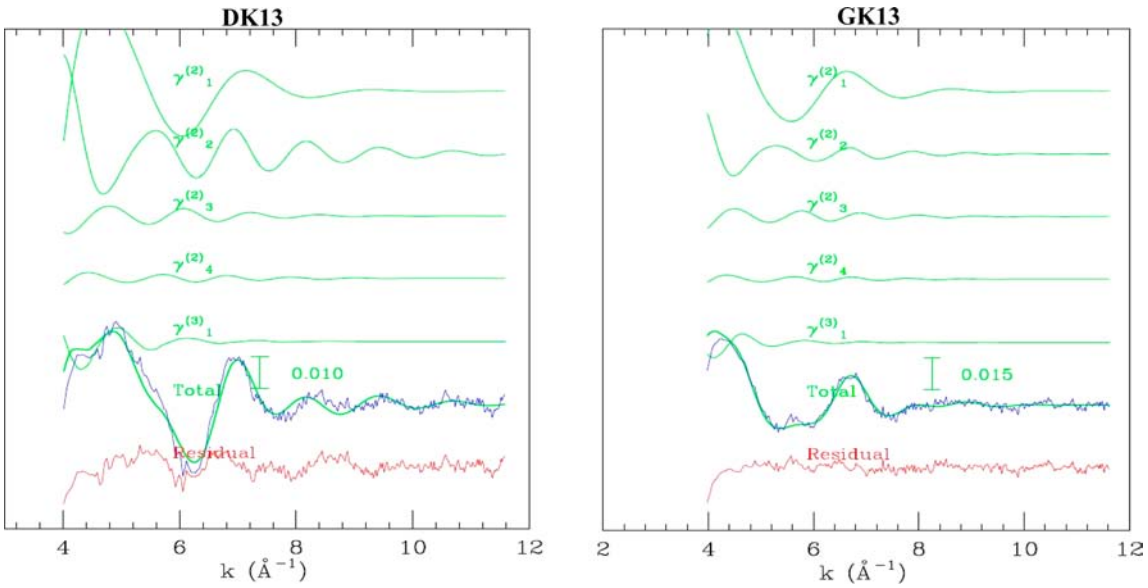

Figure 4. Different contributions to the EXAFS signals of Cu(III) (left panel) and Cu(II) (right panel) containing peptide samples.

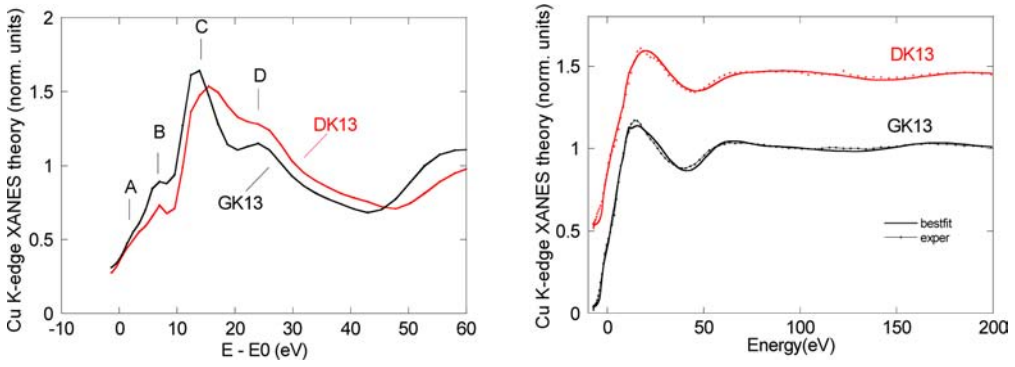

Figure 5. Left frame: Theoretical XANES spectra (without broadening) of DK13/Cu(III) and GK13/Cu(II). Right frame: Theoretical vs experimental XANES fit (after broadening) of DK13 (red) and GK13 (black) copper complexes, obtained by refining structural and nonstructural parameters.

dx.doi.org/10.1021/ic201469h | *Inorg. Chem.* 2012, 51, 7969−7976

Table 2. Essential Parameters of the XANES Fit (Errors in Brackets)

sample	sq. residual[a]	overlap factor (%)	V_0imp (eV)	⟨CuN⟩ (Å)[b]	⟨Cu−C⟩ (Å)[b,c]
DK13	1.9447	4.95 (0.09)	−11.98 (2.0)	1.80 (0.04)	2.84 (0.08)
				1.78 (0.02)	*2.89 (0.02)*
GK13	1.4712	1.34 (0.02)	−8.92 (2.0)	1.91 (0.02)	2.94 (0.02)
				1.92 (0.02)	*2.97 (0.02)*

[a]The definition of the square residual is given in ref 15. [b]For comparison purpose, also the EXAFS derived values are given in italics. [c]This value represent an average of the eight shortest Cu−C distances.

CONCLUSIONS

Comparison of XANES pre-edge peak features with those of Cu model compounds allowed to determine the Cu oxidation state in the three peptides: Cu is purely divalent in GK13, trivalent in DK13, at least in the detection limits of the method, whereas LK13 forms complexes both with Cu(II) and Cu(III) ions. Spectroscopic UV−vis data confirm these results except for peptide **1** where a small amount of Cu(II) could be still identified. Notably, also edge energies and the Cu−N distances derived independently by GNXAS (1.79 Å and 1.90 Å in the EXAFS range) and MXAN (1.80 Å and 1.91 Å in the XANES range) for DK13 and GK13 respectively are consistent with the XANES determined Cu oxidation states. Finally, the good agreement between structural data of the Cu(III) local environment determined independently by EXAFS and XANES testifies the reliability of the determined Cu location and coordination geometry.

Preliminary theoretical XANES spectra (data not shown) calculated using the MXAN code in a different way (i.e., by fixing the optimized distances and releasing angular parameters) suggest that the CuN_4 unit is not perfectly planar but form a distorted pyramid. The Cu(III) is bonded to the four amidic nitrogens, giving rise a *quasi*-planar square structure. In fact the deviation from the planar coordination is very small (the angle N−Cu−N of two opposite nitrogens is about 170°) and the pyramidal structure is near to be flat. The proposed structures for DK13/Cu(III) and GK13/Cu(II) are depicted in Figures 6 and 7.

The absence in GK13 of the Cu(III) coordinated species reported in Figure 6 for DK13, although peptides (**1**) and (**3**) have the same size of the peptide ring, might be tentatively explained by the control of the backbone-hanging imidazole side chains coming from D- and L-histidines, which are not present in compound (**3**). Surprisingly, it also appears that the chirality of His residues may play a role in the Cu(II) → Cu(III) oxidation pattern as peptide (**2**)/Cu(II) complex, that contains two L-histidines, was oxidized only in part. The addition of imidazole itself into a solution of GK13/Cu(II) did not produce anyway the formation of the Cu(III) ions, but the spectra remain substantially unchanged respect to those collected for GK13/Cu(II) mixture. The mechanism by which the histidine residues act in creating the suitable cradle for dioxygen Cu(II) → Cu(III) formation is not clarified at this stage. A pH dependent EXAFS study in aqueous solution will be necessary for revealing in detail the role of the D- and L-histidine in cyclopeptide (**1**) and (**2**) copper complexing.

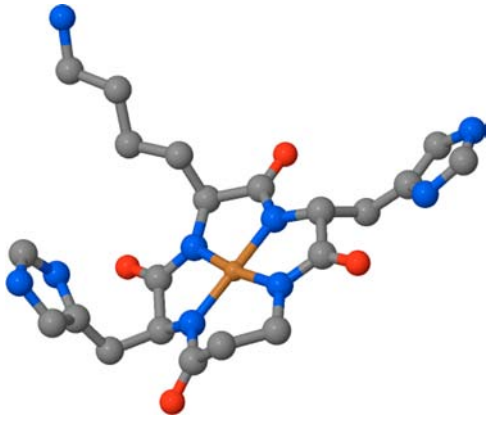

Figure 6. Proposed structure for DK13/Cu(III) complex on the basis of XANES data.

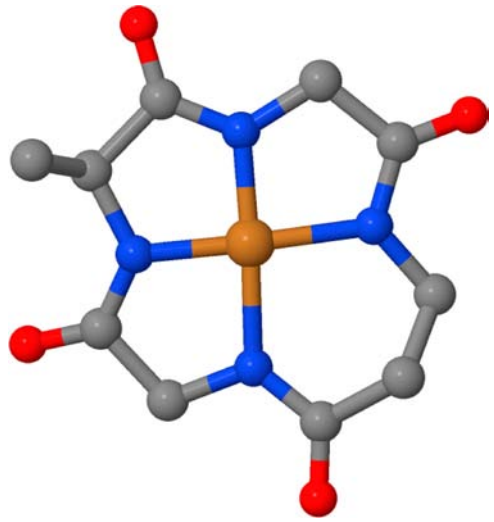

Figure 7. Proposed structure for GK13/Cu(II) complex on the basis of UV−vis data.

ASSOCIATED CONTENT

Supporting Information

Experimental procedures and characterization data. This material is available free of charge via the Internet at http://pubs.acs.org.

AUTHOR INFORMATION

Corresponding Author

*E-mail: mauro.ginanneschi@unifi.it. Phone: +39 055 457 3525. Fax: +39 055 457 3531.

Present Address

⊥Stanford Synchrotron Radiation Light Source, SLAC National Accelerator Laboratory, Menlo Park, CA 94025, USA

Notes

The authors declare no competing financial interest.

■ ACKNOWLEDGMENTS

The authors wish to thank the ID26 beamline staff (ESRF) for kind assistance during data collection. The European Synchrotron Radiation Facility (ESRF-ID26), the Ente Cassa di Risparmio di Firenze and the European Institute of Oncology are gratefully acknowledged for the financial support.

■ ABBREVIATIONS USED

DIPEA, *N*,*N*-diisopropylethylamine; DMF, dimethylformamide; EXAFS, extended X-ray absorption fine structure; HOBt, 1-hydroxybenzotriazole; NMM, *N*-methylmorpholine; SPPS, solid phase peptide synthesis; TBTU, *O*-(benzotriazol-1-yl)-*N*,*N*,*N*′,*N*′-tetramethyluronium tetrafluoroborate; TFA, trifluoroacetic acid; TIS, triisopropylsilane; XANES, X-ray absorption near edge structure

■ REFERENCES

(1) Orfei, M.; Alcaro, M. C.; Marcon, G.; Chelli, M.; Ginanneschi, M.; Kozlowski, H.; Brasun, J.; Messori, L. *J. Inorg. Biochem.* **2003**, *97*, 299−307.
(2) Jones, P. W.; Taylor, D. M.; Williams, D. R. *J. Inorg. Biochem.* **2000**, *81*, 1−10.
(3) Brasun, J.; Matera, A.; Oldziej, S.; Swiatek-Kozlowska, J.; Messori, L.; Gabbiani, C.; Orfei, M.; Ginanneschi, M. *J. Inorg. Biochem.* **2007**, *101*, 452−460.
(4) Chelli, M.; Ginanneschi, M.; Laschi, F.; Muniz-Miranda, M.; Papini, A. M.; Sbrana, G. *Spectrochim. Acta, Part A* **1999**, *55A*, 1675−1689.
(5) Sabatino, G.; Chelli, M.; Mazzucco, S.; Ginanneschi, M.; Papini, A. M. *Tetrahedron Lett.* **1999**, *40*, 809−812.
(6) Casolaro, M.; Chelli, M.; Ginanneschi, M.; Laschi, F.; Messori, L.; Muniz-Miranda, M.; Papini, A. M.; Kowalik-Jankowska, T.; Kozlowski, H. *J. Inorg. Biochem.* **2002**, *89*, 181−190.
(7) Alcaro, M. C.; Sabatino, G.; Uziel, J.; Chelli, M.; Ginanneschi, M.; Rovero, P.; Papini, A. M. *J. Pept. Science* **2004**, *10*, 218−228.
(8) Brasun, J.; Gabbiani, C.; Ginanneschi, M.; Messori, L.; Orfei, M.; Swiatek-Kozlowka, J. *J. Inorg. Biochem.* **2004**, *98*, 2016−2021.
(9) Brasuń, J.; Matera-Witkiewicz, A.; Stanislaw, O.; Pratesi, A.; Ginanneschi, M.; Messori, L. *J. Inorg. Biochem.* **2009**, *103*, 678−688.
(10) Pratesi, A.; Zanello, P.; Giorgi, G.; Messori, L.; Casini, A.; Corsini, M.; Gabbiani, C.; Orfei, M.; Rosani, C.; Ginanneschi, M. *Inorg. Chem.* **2007**, *46*, 10038−10040.
(11) Bossu, F. P.; Chellappa, K. L.; Margerum, D. W. *J. Am. Chem. Soc.* **1977**, *99*, 2195−2203.
(12) Wilke, M.; Farges, F.; Petit, P. E.; Brown, G. E.; Martin, F. *Am. Mineral.* **2001**, *86*, 714−730.
(13) Filipponi, A.; Di Cicco, A. *TASK Q.* **2000**, *4*, 575−669.
(14) Hedin, L.; Lundqvist, B. I. *J. Phys. C* **1971**, *4*, 2064−2083.
(15) Benfatto, M.; Della Longa, S. *J. Synchrotron Radiat.* **2001**, *8*, 1087−1094.
(16) Natoli, C. R.; Benfatto, M.; Della Longa, S.; Hatada, K. *J. Synchrotron Radiat.* **2003**, *10*, 26−42.
(17) Benfatto, M.; Della Longa, S.; Natoli, C. R. *J. Synchrotron Radiat.* **2003**, *10*, 51−57.
(18) Müller, J. E.; Jepsen, O.; Wilkins, J. W. *Solid State Commun.* **1984**, *42*, 4331−4343.
(19) Blackburn, N. J.; Strange, R. W.; Reedijk, J.; Volbeda, A.; Farooq, A.; Karlin, K. D.; Zubietale, J. *Inorg. Chem.* **1989**, *28*, 1349−1357.
(20) Pickering, I. J.; George, G. N.; Dameron, C. T.; Kurz, B.; Winge, D. R.; Dance, I. G. *J. Am. Chem. Soc.* **1993**, *115*, 9498−9505.
(21) Kau, L. S.; Spira-Solomon, D. J.; Penner-Hahn, J. E.; Hodgson, K. O.; Solomon, E. I. *J. Am. Chem. Soc.* **1987**, *109*, 6433−6442.
(22) DuBois, J. L.; Mukherjee, P.; Stack, T. D. P.; Hedman, B. E.; Solomon, I.; Hodgson, K. O. *J. Am. Chem. Soc.* **2000**, *122*, 5775−5787.
(23) Farges, F.; Siewert, R.; Ponader, C. W.; Brown, G. E.; Pichavant, M.; Behrens, H. *Can. Mineral.* **2006**, *44*, 755−773.
(24) Chillemi, G.; Barone, V.; D'Angelo, P.; Mancini, G.; Persson, I.; Sanna, N. J. *Phys. Chem. B* **2005**, *109*, 9186−9193.
(25) Brown, G. E.; Farges, F.; Calas, G. *Rev. Mineral. Geochem.* **1995**, *32*, 317−410.
(26) Neubecker, T. A.; Kirsey, S. T., Jr; Chellappa, K. L.; Margerum, D. W. *Inorg. Chem.* **1979**, *18*, 444−448.
(27) Aquilanti, G.; Giorgetti, M.; Minicucci, M.; Papini, G.; Pellei, M.; Tegoni, M.; Trasattic, A.; Santini, C. *Dalton Trans.* **2011**, *40*, 2764−2777.